Available online at www.sciencedirect.com

SCIENCE DIRECT®

Tetrahedron: *Asymmetry* 17 (2006) 1812–1816

Tetrahedron: *Asymmetry*

Molecular mechanism of DCR phenomenon observed in (*RS*)-1-cyclohexylethylamine–mandelic acid resolution system

Kenichi Sakai,[a,*] Rumiko Sakurai[a] and Noriaki Hirayama[b,*]

[a] *R&D Division, Yamakawa Chemical Industry Co., Ltd, Kitaibaraki, Ibaraki 319-1541, Japan*
[b] *Basic Medical Science and Molecular Medicine, Tokai University School of Medicine, Isehara, Kanagawa 259-1193, Japan*

Received 27 April 2006; revised 19 June 2006; accepted 20 June 2006

Abstract—In the resolution system of (*RS*)-1-cyclohexylethylamine (CHEA) with (*S*)-mandelic acid (MA), the DCR (dielectrically controlled resolution) phenomenon was clearly observed. (*S*)-CHEA and (*R*)-CHEA were obtained as less-soluble salts from 2-propanol ($\varepsilon = 18$) and water ($\varepsilon = 78$), respectively. Although (*S*)-MAs pack similarly in the crystals of both of the salts, the chiral spaces formed between the columns of (*S*)-MAs are significantly different in shape. The present study showed that these chiral spaces are crucial to molecular recognition and their shapes are greatly influenced by the dielectric property of the solvent employed.

1. Introduction

An enantiopure 1-cyclohexylethylamine (CHEA) is an important key compound for syntheses of several enzyme inhibitors such as an inosine monophosphate dehydrogenase inhibitor,[1] Src kinase inhibitor,[2] and a fused pyridine inhibitor.[3] Enantiopure CHEA is also applied as a resolving agent for the enantiomeric separation of chiral acids.[4] Recently, we found that CHEA can be resolved with a series of 2-phenylacetic acids such as 2-methoxy-2-phenylacetic acid (MPAA), 2-phenylpropionic acid (PPA), and mandelic acid (MA).[5] During resolution with (*S*)-MA as a resolving agent, we found that the (*R*)- and (*S*)-enantiomers were resolved from water and 2-propanol, respectively. Therefore it is of great interest to study whether the CHEA–MA system shows the DCR phenomenon or not, and we have undertaken systematic resolution experiments on this system. The salt between (*S*)-CHEA and (*S*)-MA is designated as (*S*)-CHEA–(*S*)-MA. The diastereomeric salt between (*R*)-CHEA and (*S*)-MA is designated as (*R*)-CHEA–(*S*)-MA–W because it is a hemihydrate (Scheme 1).

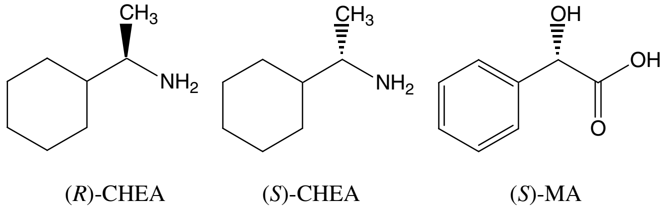

Scheme 1. Chemical structures of CHEA and MA.

2. Results and discussion

2.1. Resolution experiments, preparation of pure (*R*)-CHEA–(*S*)-MA–W and (*S*)-CHEA–(*S*)-MA salts and X-ray analysis

An equimolar resolving agent ((*S*)-MA) was used to (*RS*)-CHEA and the solvent volume was determined by the solubility of the solid substances at 50 °C in each resolution experiment. Resolution experiments using various solvents with different dielectric constants are shown in Table 1. Although the diastereomeric salts were obtained from only four solvents, the DCR phenomenon was clearly observed. The diastereomeric salts of (*S*)-CHEA and (*R*)-CHEA were obtained from 2-propanol ($\varepsilon = 18$) and water ($\varepsilon = 78$), respectively. The single crystals of (*S*)-CHEA–(*S*)-MA and (*R*)-CHEA–(*S*)-MA–W were recrystallized from the solvents used for the resolution.

In order to elucidate the molecular mechanism of the DCR phenomenon, X-ray analysis was undertaken. Data were

---

[*] Corresponding authors. E-mail addresses: kensakai@cd6.so-net.ne.jp; hirayama@is.icc.u-tokai.ac.jp

0957-4166/$ - see front matter © 2006 Elsevier Ltd. All rights reserved.
doi:10.1016/j.tetasy.2006.06.037

Table 1. Resolution of (*RS*)-CHEA with (*S*)-MA in various solvents: effect of the dielectric property of the solvent

Solvent	ε	Solvent volume versus (*RS*)-CHEA (w/w)	Yield versus (*RS*)-CHEA (%)	de%	Absolute configuration
Chloroform	5	11.2	Not crystallized		
99% Chloroform	6	11.2	Not crystallized		
2-PrOH	18	6.5	3	24	*S*
97% 2-PrOH	20	5.0	20	16	*S*
MeOH	33	2.0	Not crystallized		
81% EtOH	34	2.1	Not crystallized		
88% MeOH	38	2.0	Solidified		
		3.0	Not crystallized		
DMSO	49	2.2	9	30	*S*
50% EtOH	51	2.5	Not crystallized		
40% MeOH	60	1.0	Solidified		
		2.0	Not crystallized		
Water	78	12.0	7	91	*R*

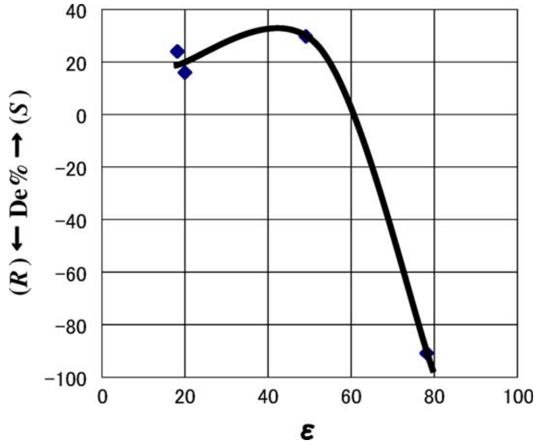

collected on a Rigaku RAPID diffractometer equipped with Cu-Kα radiation and processed using the Process Auto package.[6] The structures were solved by direct methods [SIR92].[7] Full-matrix least squares refinement was carried out using observed reflections with $I > 2.00\sigma(I)$. The crystallographic data and refinement results are summarized in Table 2. All non-hydrogen atoms were refined using anisotropic displacement parameters. For both crystals, all H atoms were located from difference Fourier synthesis and refined by the riding model. The absolute configurations were fixed to the known ones in both crystal structures and not reconfirmed by the X-ray analyses independently. All of the calculations were performed using the software system crystal structure.[8] Crystallographic data for (*S*)-CHEA–(*S*)-MA and (*R*)-CHEA–(*S*)-MA–W have been deposited with Cambridge Crystallographic Data

Table 2. Crystal and experimental data

	(*S*)-CHEA–(*S*)-MA	(*R*)-CHEA–(*S*)-MA–W
Formula	$C_8H_{17}N{\cdot}C_8H_8O_3$	$C_8H_{17}N{\cdot}C_8H_8O_3{\cdot}0.5H_2O$
Formula weight	279.38	288.39
Crystal system	Orthorhombic	Monoclinic
Space group	$P2_12_12_1$, $Z = 4$	$C2$, $Z = 4$
a	5.62(1) Å	16.64(3) Å
b	15.45(3) Å	6.32(1) Å
c	19.26(4) Å	14.64(3) Å
β	—	96.4(1)°
V	1670(6) $Å^3$	1529(4) $Å^3$
Dx	1.111 g/cm^3	1.252 g/cm^3
No. of observations ($I > 2.00\sigma(I)$)	535	1936
θ_{max} with Cu-Kα	68.14°	68.25°
R ($I > 2.00\sigma(I)$)	0.052	0.062
$(\Delta/\sigma)_{max}$	0.001	0.000
$(\Delta\rho)_{max}$	0.18 e/$Å^3$	0.35 e/$Å^3$
$(\Delta\rho)_{min}$	−0.17 e/$Å^3$	−0.25 e/$Å^3$

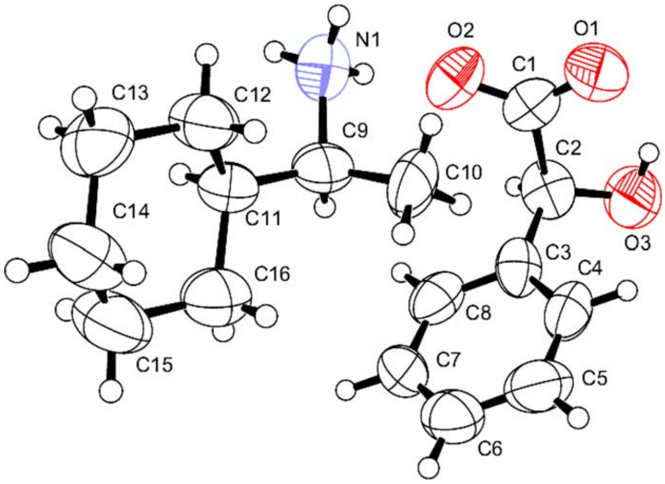

Figure 1. Molecular structures of CHEA and MA in the (*S*)-CHEA–(*S*)-MA crystal.

Centre as supplementary publication numbers CCDC 234886 and 234885, respectively.

2.2. Molecular structure of CHEA and MA in the crystals

The molecular structures of CHEA and MA in the crystal (*S*)-CHEA–(*S*)-MA depicted by ORTEPIII[9] are shown in Figure 1 with the atomic labeling system. The selected bond lengths, angles and torsion angles are given in Table 3.

Two C–O bond lengths in MA are asymmetric in (*S*)-CHEA–(*S*)-MA. On the other hand, they are symmetrical in (*R*)-CHEA–(*S*)-MA–W. The (*S*)-MA molecules in both crystal structures take relatively different conformations. The torsion angles of O3–C2–C3–C4 in (*S*)-CHEA–(*S*)-MA and (*R*)-CHEA–(*S*)-MA–W are 38(1)° and 7.2(5)°, respectively. CHEA adopts a similar chair conformation in both crystal structures. The conformations of the ethylamine moieties, however, are significantly different. Although the torsion angles of N1–C9–C11–C12 agree within experimental error in both crystal structures, the torsion angles of N1–C9–C11–C16 are significantly different with the values being 173(1) and −66.8(5) in (*S*)-CHEA–(*S*)-MA and (*R*)-CHEA–(*S*)-MA–W, respectively. These geometrical differences indicate that chiral selectors and target molecules should undergo structural change appreciably in order to realize optimum molecular recognition. Only a molecular recognition with sufficient molecular interactions can produce crystals which can be purely separated.

Table 3. Selected bond lengths (Å), bond angles (°) and torsion angles (°)

	(*S*)-CHEA–(*S*)-MA	(*R*)-CHEA–(*S*)-MA–W
O(1)–C(1)	1.21(2)	1.228(5)
O(2)–C(1)	1.26(2)	1.228(6)
O(3)–C(2)	1.42(1)	1.396(6)
N(1)–C(9)	1.54(1)	1.466(5)
O(1)–C(1)–O(2)	127(1)	124.0(4)
O(1)–C(1)–C(2)	113(1)	119.1(4)
O(2)–C(1)–C(2)	118(1)	117.0(3)
O(3)–C(2)–C(1)	111(1)	109.4(3)
O(3)–C(2)–C(3)	111(1)	110.8(4)
N(1)–C(9)–C(10)	108.7(9)	108.5(3)
N(1)–C(9)–C(11)	109.1(8)	112.3(3)
O(1)–C(1)–C(2)–O(3)	−18(1)	−17.3(5)
O(1)–C(1)–C(2)–C(3)	104(1)	105.9(5)
O(2)–C(1)–C(2)–O(3)	163(1)	161.8(4)
O(2)–C(1)–C(2)–C(3)	−73(1)	−75.0(5)
O(3)–C(2)–C(3)–C(4)	38(1)	7.2(5)
O(3)–C(2)–C(3)–C(8)	−144(1)	−170.8(4)
N(1)–C(9)–C(11)–C(12)	−61(1)	60.1(5)
N(1)–C(9)–C(11)–C(16)	173(1)	−66.8(5)

Crystal structures of (*S*)-CHEA–(*S*)-MA and (*R*)-CHEA–(*S*)-MA–W are compared in Figure 2. (*S*)-MA and CHEA are depicted by van der Waals spheres and sticks, respectively. Water molecules are colored in green. In both crystal structures, the (*S*)-MA molecules pack similarly and build up a chiral space where CHEA molecules are recognized.

In the crystal structure of (*S*)-CHEA–(*S*)-MA (Fig. 2a), the width of the chiral space is relatively wide but only (*S*)-CHEA can be accommodated in it. The width of the chiral space represented by the separation between the C1 atom of (*S*)-MA and the center of the phenyl group of another (*S*)-MA that locates on the opposite side of the chiral space is 9.33 Å; the width is shown by yellow dotted line. In the crystal structure of (*R*)-CHEA–(*S*)-MA–W (Fig. 2b), (*S*)-

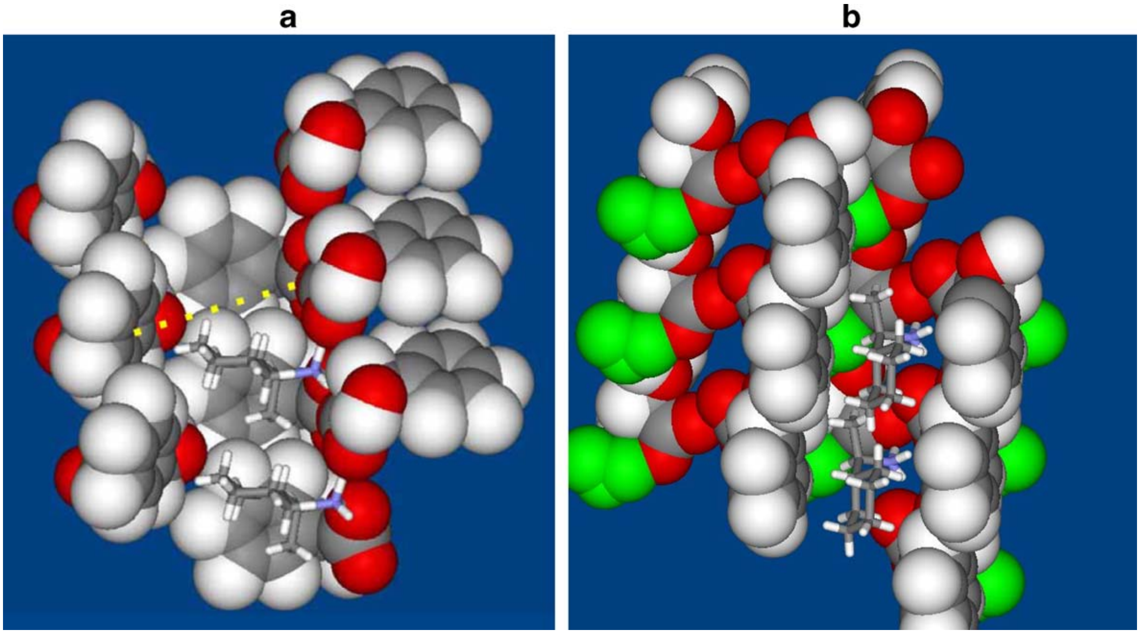

Figure 2. Crystal structures of CHEA–MA system viewed along the *c* axis. (a) (*S*)-CHEA–(*S*)-MA: MAs are drawn by van der Waals radii and CHEA sticks. Oxygen, nitrogen, carbon and hydrogen atoms are shown in red, blue, gray, and white, respectively. (b) (*R*)-CHEA–(*S*)-MA–W: MAs are drawn by van der Waals radii and CHEA sticks. Oxygen, nitrogen, carbon and hydrogen atoms are shown in red, blue, gray and white, respectively. Oxygen and hydrogen atoms of water molecules are depicted by van der Waals radii in green.

MA forms columns perpendicular to the *a* axis. Therefore, the width of the chiral space is roughly a half length of the *a* axis, that is, 8.32 Å.

The hydrophilic columns and layers in both crystal structures are highlighted in Figure 3. Oxygen and nitrogen atoms are emphasized by van der Waals spheres. In Figure 3a, the crystal structure of (*R*)-CHEA–(*S*)-MA–W is viewed along the *b* axis. The hydrophilic layers extend along the *b* axis and are perpendicular to the *c* axis. The separation between the hydrophilic layers is 14.64 Å. The crystal structure of (*S*)-CHEA–(*S*)-MA viewed along the *a* axis is shown in Figure 3b. The hydrophilic columns extend along the *a* axis and they do not stack in parallel to each other. The spacing between the centers of the nearest-neighbor columns is 9.63 Å. Although the chiral space in (*R*)-CHEA–(*S*)-MA–W is narrower than that in (*S*)-CHEA–(*S*)-MA, the separation of the hydrophilic columns in the former crystal is significantly wider than that in the latter crystal.

In Table 4, hydrogen bonds in both crystal structures are given. In the crystal structure of (*S*)-CHEA–(*S*)-MA, O2 is involved in three hydrogen bonds with N1, whereas O1

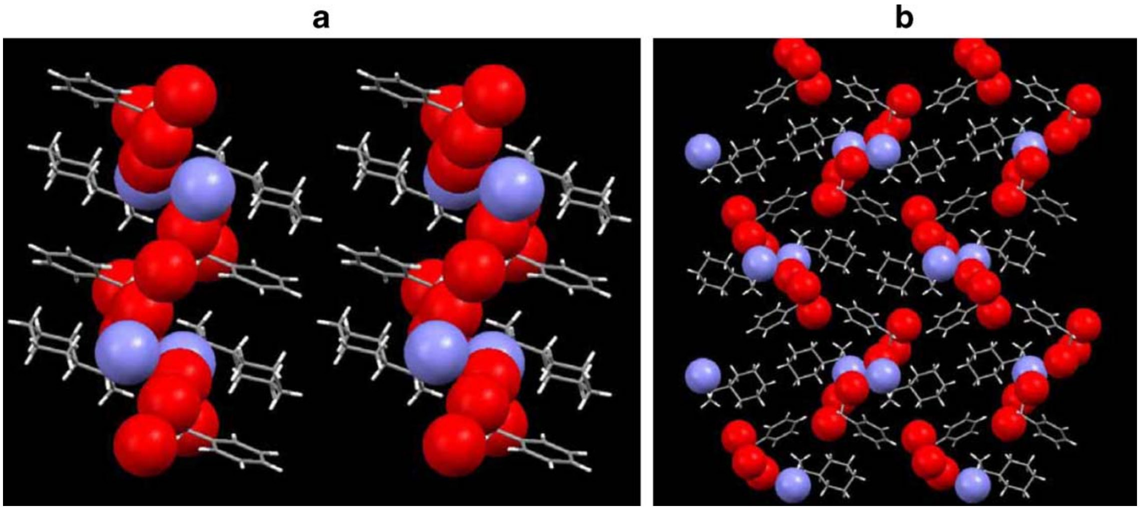

Figure 3. Hydrophilic columns and layers: (a) (*R*)-CHEA–(*S*)-MA–W viewed along the *b* axis. Oxygen and nitrogen atoms are depicted by van der Waals radii in red and blue, respectively. Other atoms are drawn by sticks; (b) (*S*)-CHEA–(*S*)-MA viewed along the *a* axis. Oxygen and nitrogen atoms are depicted by van der Waals radii in red and blue, respectively. Other atoms are shown by sticks.

Table 4. Hydrogen bonds

Donor–H· · ·acceptor	[Symmetry code]	D–H	H· · ·A	D· · ·A	D–H· · ·A
(S)-CHEA–(S)-MA					
Intra					
O(3)–H(7)· · ·O(1)	[ ]	0.90	1.91	2.640(14)	137
N(1)–H(23)· · ·O(1)	[3566]	0.91	2.04	2.835(15)	146
N(1)–H(23)· · ·O(2)	[3566]	0.91	2.58	3.429(17)	157
N(1)–H(24)· · ·O(2)	[3466]	0.91	1.88	2.777(16)	168
N(1)–H(25)· · ·O(2)	[ ]	0.90	2.00	2.896(13)	174
(R)-CHEA–(S)-MA–W					
O(3)–H(7)· · ·O(4)	[1565.03]	1.06	1.80	2.719(7)	143
N(1)–H(23)· · ·O(1)	[1545.02]	0.81	2.13	2.787(7)	138
N(1)–H(23)· · ·O(3)	[1545.02]	0.81	2.44	3.151(8)	148
N(1)–H(24)· · ·O(2)	[ ]	0.98	1.84	2.783(7)	160
N(1)–H(25)· · ·O(1)	[4244.02]	0.97	1.93	2.852(7)	156
O(4)–H(26)· · ·O(2)	[2354.02]	1.07	1.65	2.677(7)	158

Symmetry code
[3566.] = $1/2 + x, 3/2 - y, 1 - z$.
[3466.] = $-1/2 + x, 3/2 - y, 1 - z$.
[1545.] = $x, -1 + y, z$.
[4244.] = $-5/2 - x, -1/2 + y, -1 - z$.
[1565.] = $x, 1 + y, z$.
[2364.] = $-2 - x, 1 + y, -1 - z$.
[2354.] = $-2 - x, y, -1 - z$.

is involved in one hydrogen bond with N1. In the crystal structure of (*R*)-CHEA–(*S*)-MA–W, however, O1 is involved in two hydrogen bonds with N1. The O2 is involved in one hydrogen bond with the N1 and one hydrogen bond with the water molecule. It is interesting to note that O3 is involved in intermolecular hydrogen bonds in (*R*)-CHEA–(*S*)-MA–W, but not in (*S*)-CHEA–(*S*)-MA.

The markedly different hydrogen-bond schemes observed in two crystal structures indicate that the dielectric property of the solvent that significantly influences the states of carboxylate group should also play an important role in DCR.

2.3. Molecular mechanism of DCR phenomenon

The crystal structures described above illustrate a molecular mechanism of the DCR phenomenon observed in the (*RS*)-CHEA–(*S*)-MA resolution system. In the solution, (*S*)-MA is considered to be highly inclined to aggregate to form similar columns because (*S*)-MA packs in a similar fashion in both crystal structures. Between the columns, chiral spaces are formed. In a solvent with a smaller dielectric constant, the columns come close together to form a chiral space where (*S*)-CHEA is better recognized than (*R*)-CHEA. In the solvent with a smaller dielectric constant, the O2 of MA highly tends to form hydrogen bonds with the ammonium ion. In the chiral space the structure of (*S*)-CHEA can fulfill this requirement and only (*S*)-CHEA can be recognized in this chiral space. In the solvent with a larger dielectric constant, however, the separation between the hydrophilic layers increases because of reduced electrostatic interactions between them. As water molecules must be incorporated between the columns to realize the close packing, hydrophilic layers are now formed instead of hydrophilic columns. The chiral space is formed between hydrophobic walls with a hydrophilic floor and ceiling as shown in Figure 2b. The width of the chiral space is narrow in this case. In the solvent with a larger dielectric constant, O1, O2, and O3 can be equally involved in the intermolecular hydrogen bonds with the N atom. Accordingly, the structure of (*R*)-CHEA is more preferable to (*S*)-CHEA in this chiral space. In addition, both the CHEA and MA molecules can undergo conformational changes to obtain an optimum fit into the chiral space in order to form crystals to be precipitated.

The present study has demonstrated that the DCR phenomenon observed in the (*RS*)-CHEA–(*S*)-MA resolution system is due to the change of the chiral spaces directly caused by the dielectric properties of the solvents used in the resolution processes.

3. Experimental

3.1. Resolution procedure

(*RS*)-1-Cyclohexylethylamine **1**, (*S*)-mandelic acid **2** (>99.5% ee), was made by Yamakawa Chemical (Tokyo). A typical experimental procedure is the same as described in our previous report.[5] Dielectric constants of the mixed solvents were calculated based on the literature.[10]

3.2. Determination of diastereomeric excess of CHEA

The enantiomeric purity of CHEA presented in the salt was based on the enantiomeric excess of the amine liberated from the salt. Enantiomeric excess of CHEA was determined directly by HPLC using a SUMICHIRAL OA-4600 column (ID 4.6 mm × 250 mm). Analytical conditions for the HPLC were as follows: eluent: *n*-hexane + ethanol (98/20), 1.0 mL/min, 40 °C, detected at 254 nm; injection sample 10 μL (10 mg/10 mL); retention times: the (*S*)-enantiomer 18.5 min, the (*R*)-enantiomer 17.1 min. A sample for chiral purity analysis by HPLC was treated with 3,5-dinitrobenzoyl chloride (DNB) prior to injection.

References

1. Iwanowicz, E. J.; Dhar, M.; Leftheris, K.; Liu, C.; Mitt, T.; Watterson, S. H.; Barrish, J. C. U.S. Patent 6,420,403, 2002.
2. Armstrong, H. M.; Beresis, R.; Goulet, J. L.; Holmes, M.; Hong, X.; Mills, S. G.; Parsons, W. H.; Sinclair, P. J.; Steiner, M. G.; Wong, F.; Zaller, D. M. U.S. Patent 6,498,165, 2002.
3. Macor, J. E. U.S. Patent 6,326,379, 2001.
4. (a) Yamada, S.; Seki, M.; Yoshioka, R.; Shibatani, T., Japan Patent Kokai 1999-322668; (b) Seki, M.; Yamada, S.; Kuroda, T.; Imashiro, R.; Shimizu, T. *Synthesis* **2000**, 1677.
5. Sakai, K.; Yokoyama, M.; Sakurai, R.; Hirayama, N. *Tetrahedron: Asymmetry* **2006**, *17*, 1541–1543.
6. Process-Auto. Automatic Data Acquisition and Processing Package for Imaging Plate Diffractometer, Rigaku, Tokyo, Japan, 1998.
7. Alltomare, A.; Cascarano, G.; Giacovazzo, C.; Guagliardi, A.; Burla, M.; Polidori, G.; Camalli, M. *J. Appl. Crystallgr.* **1994**, *27*, 435.
8. CrystalStructure Ver. 3.6.0, Crystal Structure Analysis Package, Rigaku and Rigaku/MSC, 2004.
9. Burnett, M. N.; Johnson, C. K. ORTEP-III: Oak Ridge Thermal Ellipsoid Plot Program for Crystal Structure Illustration, Oak Ridge National Laboratory, Report ORNL-6895, 1996.
10. The values of dielectric constants of mixed solvents were calculated as the weighted average of the mixture components, alcohol and water, based on the literatures; (a) Jouyban, A.; Soltanpour, S.; Chan, H.-K. *Int. J. Pharm.* **2004**, *269*, 353–360; (b) Prakongpan, S.; Nagai, T. *Chem. Pharm. Bull.* **1984**, *32*, 340–343.